DISCHARGE MORPHOLOGY AND SPECTRAL DIAGNOSTIC OF A SERRATED DBD PLASMA ACTUATOR DEDICATED TO AERODYNAMIC FLOW CONTROL APPLICATIONS

K. CHATELAIN[1], R. JOUSSOT[2], A. LEROY[1]*, V. LAGO[2], H. RABAT[3], D. HONG[3]

[1] PRISME, Univ. Orléans, INSA-CVL, UPRES 4229, F-45072, Orléans, France
[2] ICARE, CNRS, UPR 3021, F-45071, Orléans, France
[3] GREMI, Univ. Orléans, CNRS, UMR 7344, F-45067, Orléans, France
*annie.leroy@univ-orleans.fr

ABSTRACT

The serrated DBD plasma actuator configuration, with the exposed electrode having a sawtooth edge, was compared to the standard one (i.e. with strip electrodes) in order to highlight plasma channels induced by the serration. The differences in the plasma morphology and properties between these configurations were investigated by using optical diagnostics, in quiescent air. Images of the discharge were recorded by an ICCD camera, with and without narrow-band filters and an optical emission spectrometer was used to measure the spectral bands of N_2 and N_2^+, allowing the rotational temperatures to be estimated.

1. INTRODUCTION

Plasma actuators applied for aerodynamic flow control is an expanding area of research. These electrohydrodynamic devices are well adapted for active control because of their interesting properties such as total electric control, no moving parts and fast response time. Since several years many studies are carried out on the use of DBD plasma devices applied to subsonic flow modification. Investigations focused on enhanced understanding of their physical characteristics, the coupling with the air flow and optimization. For some of the aerodynamic control applications, it can be interesting to promote three-dimensional ionic wind. As proposed in Joussot *et al.*[1], the serrated plasma actuator configuration, with the exposed electrode having a sawtooth edge, allows this kind of induced flow pattern. In addition, the maximal velocity of the induced ionic wind is also increased.

Investigation of the plasma properties of the serrated plasma actuator configuration in quiescent air, using ICCD camera with narrow-band filter (NBF) and optical emission spectrometer, was performed and main results are presented in this paper. Optical emission spectroscopy (OES) measurements showed that the plasma light emission is dominated by the spectral bands corresponding to the transition of the N_2(C $^3\Pi_u^+$-B $^3\Pi_g^+$) second positive system at $\lambda = 337.14\,\mathrm{nm}$. Some molecular bands of the N_2^+(B $^2\Sigma_u^+$-X $^2\Sigma_g^+$) first negative system at $\lambda = 390.4\,\mathrm{nm}$ are also present. In order to highlight the plasma channels induced by the serration, a comparison with the plasma induced by a standard DBD configuration (i.e. with strip electrodes) is performed, considering similar electrical operating parameters. After a brief description of the the experimental set-up presentation, main results related to the differences of the plasma morphology between both configurations are presented and discussed.

2. EXPERIMENTAL SET-UP

Two sinusoidally driven DBD actuator configurations are considered, namely, the serrated plasma actuator configuration [1], with the exposed electrode having a sawtooth edge (figure 1), and the linear one (i.e. with strip electrodes). The grounded electrode was not modified. In both cases, the actuator is made of two metallic electrodes separated by a dielectric panel, consisting of three layers of two dielectric materials: a $500\,\mu\mathrm{m}$ thick Mylar sheet was placed between two Kapton sheets ($55\,\mu\mathrm{m}$ thick). The electrodes were made of adhesive copper foil tape. The upper exposed electrode is connected to an AC power supply; the lower one is grounded directly or via a measurement component. Kapton is used to encapsulate the grounded electrode in order to inhibit plasma formation on this side.

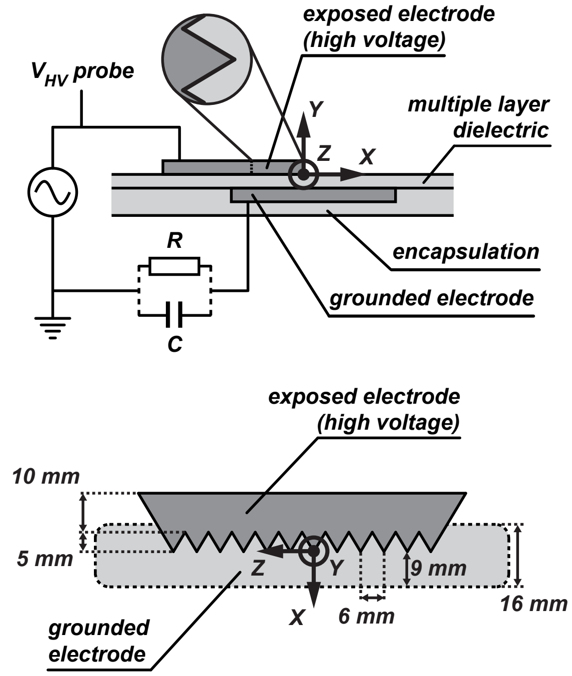

Fig. 1: Schematics of the serrated plasma actuator design

Images of the discharge are recorded by an intensified CCD camera (Andor iStar DH734) equipped with a VUV lens of 90 mm in focal length ($f/4$). The optical axis of this device was perpendicular to the plasma actuator surface. The camera was triggered using a pulse synchronized with the high voltage so that the discharge was imaged during both positive- and negative-going half-cycles. Two NBF were used in order to investigate discrepancies in the light emission between N_2 (337 nm-NBF, 20 nm-FWMH) and N_2^+ (390 nm-NBF, 20 nm-FWMH). OES was performed by collecting the light emitted from the plasma by means of a UV lens collection system focusing the maximum intensity at the entry slit of the F1500 spectrometer (see Lago *et al.*[2] for further details). The view field of the optical collection system is small enough to cover only the spot light at the tip of a tooth in the case of the serrated design. For the linear design, the light emitted just downstream the exposed electrode was recorded. The rotational temperature (T_r) is estimated from the fitting of experimental spectra with home made simulated spectra.

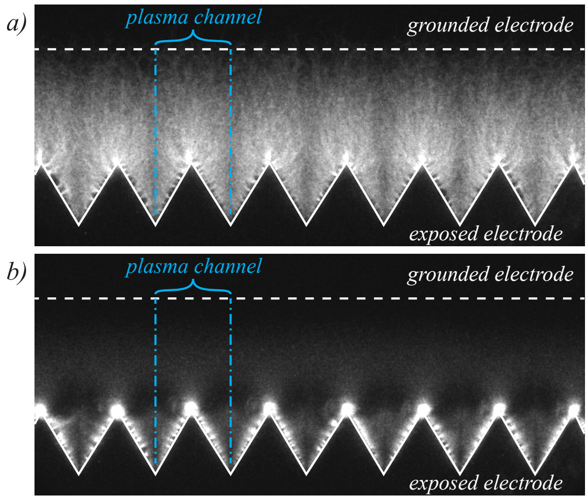

Fig. 2: Discharge images of the serrated design during: (a) positive-going and (b) negative-going half-cycles; $V_{HV} = 10\,\mathrm{kV}$ and $f_{HV} = 1\,\mathrm{kHz}$, without NBF

3. RESULTS

Two distinct regimes of a surface DBD discharge, depending on the exposed electrode polarity, were observed whatever the configuration tested. Figure 2 shows images (averaged on 10 cycles) of the discharge during positive- and negative-going half-cycles for the serrated design. The micro discharges exhibited the characteristic structures reported in the literature [3]. During the positive half-cycle, streamers propagated on the actuator surface from bright spots (corona zone) on the exposed electrode [3]. Streamers appeared as long, thin and discrete filaments spreading over the dielectric with highly filamentary paths. Due to the serrated design of the exposed electrode, the streamers had a curved shape when approaching a neighbouring tooth [1]. During the negative half-cycle, the discharge was diffuse and micro discharges appeared as corona-type plasma, emanating from discrete locations. The micro discharges propagated with a plume shape, and could take on a curved shape like the positive filaments. For each tooth of the serrated design, the discharge was self-limited, in the transverse direction, into an area delimited by two longitudinal straight axes (along the X-direction) aligned on each root [1], which outlined each plasma channel. During the negative-going half-cycle, an intense bright spot was located at the tip of each tooth due to the increase in the local electric field induced by the serration, then the plasma spread over the dielectric surface with a large plume shape.

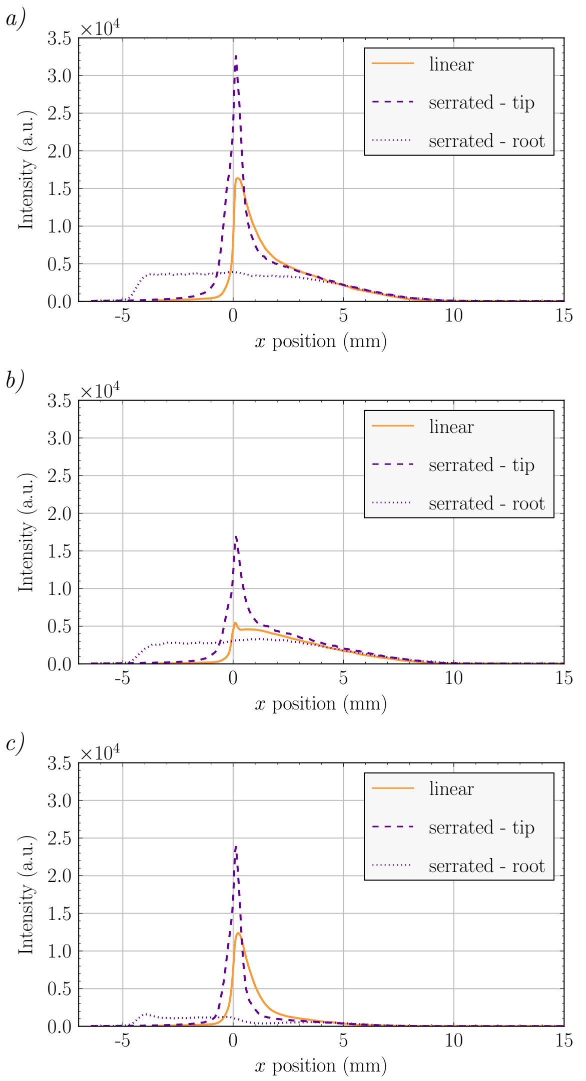

Fig. 3: Longitudinal distribution of discharge-light emission without NBF, during: (a) a 1 ms-period, (b) positive-going and (c) negative going half-cycle; $V_{HV} = 10\,\mathrm{kV}$ and $f_{HV} = 1\,\mathrm{kHz}$

The spanwise-averaged longitudinal distribution of the light intensity emitted by the plasma is calculated from the discharge images recorded with the ICCD camera, as showed on figure (Fig. 3). The shape of the longitudinal light emission profile is similar between the two configurations (for the distribution aligned with a tip of the serrated design) and this whatever the integration time is (1 ms, positive- or negative-going half-cycle), but the maximum light intensity of the serrated design is about two times the one of the linear design. At the root of the serrated design, the light-emission is faint because the probability of the plasma to reach this position is the smallest [1]. In addition, the light-emission is always higher during the negative-going half-cycle, whatever the design. For both designs, the maximum light intensity increases with the applied voltage (Fig. 4) and the light-emission intensity is always higher with the serrated design than with the linear one. However, despite the brighter plasma induced with the serrated design, the time-averaged plasma length L_p deduced from images as reported in Kriegseis *et al.*[4] is similar for both designs (Fig. 5). This last observation shows that the extent is due the intrinsic plasma properties like the time of life of the formed species and not to the plasma actuator geometry. Nevertheless the efficiency of the plasma actuator in terms of ionic wind seems directly linked to the plasma light emitted because this is related to the electron density which increases with the applied voltage.

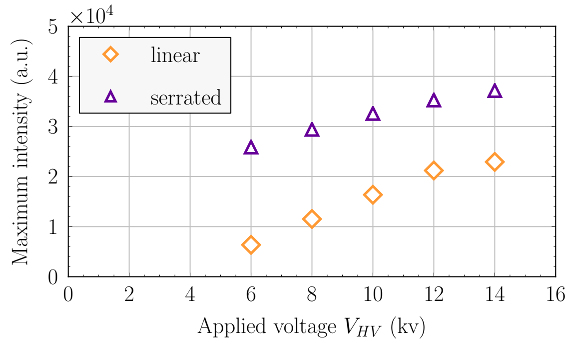

Fig. 4: Maximum value of the longitudinal distribution of discharge-light emission without NBF during a 1 ms-period according to the applied voltage V_{HV} ($f_{HV} = 1\,\mathrm{kHz}$)

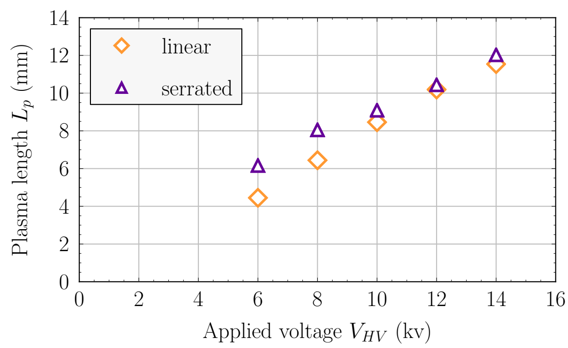

Fig. 5: Time-averaged plasma length L_p according to the applied voltage V_{HV} ($f_{HV} = 1\,\mathrm{kHz}$)

As mentioned in Dong *et al.*[5] for a linear design, only nitrogen electronic excited systems were revealed in the 275-900 nm wavelength range, such as the first negative system of $N_2^+(B)$ due to its abundance arising from direct electron ionization of nitrogen, and the second positive system of $N_2(C)$ which is populated through direct electron impact of the ground state. The estimation of the gas temperature can be deduced from the rotational temperatures which have been determined from N_2 and N_2^+ spectra (Tab. 1).

Actuator type	T_{rot,N_2} (K)	T_{rot,N_2^+} (K)
linear	445 ± 5	–
serrated (tip)	520 ± 5	962 ± 7
Actuator type	I_{N_2} (a.u.)	$I_{N_2^+}$ (a.u.)
linear	0.24	0.01
serrated (tip)	3.26	0.24

Tab. 1: Spectroscopy emission measurements for $V_{HV} = 10\,\text{kV}$ *and* $f_{HV} = 1\,\text{kHz}$

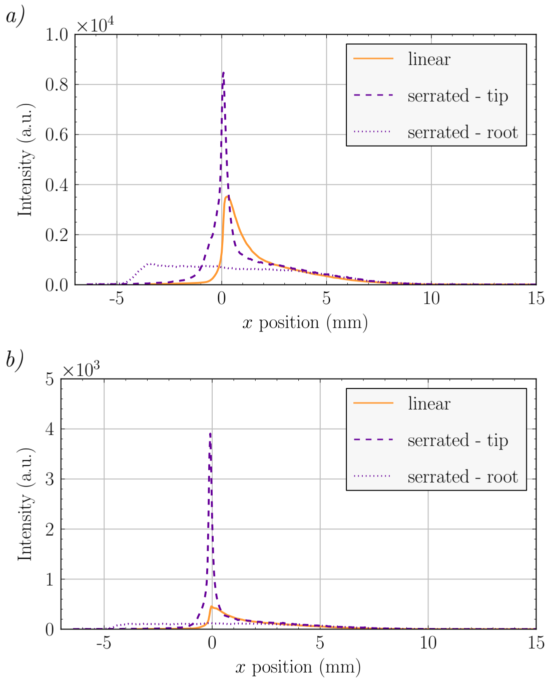

Fig. 6: Longitudinal distribution of discharge-light emission during a 1 ms-*period with: (a)* 337 nm-*NBF and (b)* 390 nm-*NBF;* $V_{HV} = 10\,\text{kV}$ *and* $f_{HV} = 1\,\text{kHz}$

An increase in the gas temperature was observed at the tooth tips for the serrated design. In addition, a difference in T_r between N_2 and N_2^+ was observed for the serrated design, meaning that the plasma is in a non-equilibrium state. For the linear design, T_r could be not calculated for N_2^+ because its light emission was very weak (Fig. 6(*b*)). The maximum line intensity (Tab. 1), representing the density of excited species N_2(C) and N_2^+(B), confirmed the results obtained by comparing the longitudinal distribution of the light emission. Indeed, the bright N_2^+(B)-emission intensity measured at the tip for the serrated design was similar to the N_2(C)-emission intensity of the linear design. The serration seems to highly increase the creation of ionized species at the tip, explaining why the longitudinal velocity value of the ionic wind is higher than the one of the linear design [1].

4. CONCLUSIONS

A serrated DBD plasma actuator, with the exposed electrode having a sawtooth edge, was compared to a standard one (i.e. with strip electrodes). Discharge images enable the longitudinal distribution of light emission to be calculated. The maximum light intensity is higher with the serrated design over the range of voltage tested. However, the plasma length remains similar between both configurations. Temperature measurements made by OES show that the gas temperature is increased at each tooth tip of the serrated design.

ACKNOWLEDGMENTS

Romain Joussot's fellowship is provided by the French Government's Investissement d'Avenir program: Laboratoire d'Excellence CAPRYSSES (ANR-11-LABX-0006-01). Additional funding is provided by the Région Centre through the PASS project (convention no. 00078782).

REFERENCES

[1] R. Joussot, A. Leroy, R. Weber, H. Rabat, S. Loyer and D. Hong, "Plasma morphology and induced airflow characterization of a DBD actuator with serrated electrode", J. Phys. D Appl. Phys., **46**(12), 125204, 2013

[2] V. Lago, R. Joussot and J.-D. Parisse, "Influence of the ionization rate of a plasma discharge applied to the modification of a supersonic low Reynolds number flow field around a cylinder", J. Phys. D Appl. Phys., **47**(12), 125202, 2014

[3] D. M. Orlov, G. I. Font and D. Edelstein, "Characterization of discharge modes of plasma actuators", AIAA J., **46**(12), pp. 3142–3148, 2008

[4] J. Kriegseis, B. Möller, S. Grundmann and C. Tropea, "Capacitance and power consumption quantification of dielectric barrier discharge (DBD) plasma actuators", J. Electrostat., **69**(4), pp. 302-312, 2011

[5] B. Dong, J.-M. Bauchire, J.-M. Pouvesle, P. Magnier and D. Hong, "Experimental study of a dbd surface discharge for the active control of subsonic airflow", J. Phys. D Appl. Phys., **41**, 155201, 2008